Compression of Surface Registration using Beltrami Coefficients

L.M. Lui, T.W. Wong, P.M. Thompson, T.F. Chan, X.F. Gu, S.T. Yau

Abstract

Surface registration is widely used in machine vision and medical imaging, where 1-1 correspondences between surfaces are computed to study their variations. Surface maps are usually stored as the 3D coordinates each vertex is mapped to, which often requires lots of storage memory. This causes inconvenience in data transmission and data storage, especially when a large set of surfaces are analyzed. To tackle this problem, we propose a novel representation of surface diffeomorphisms using Beltrami coefficients, which are complex-valued functions defined on surfaces with supreme norm less than 1. Fixing any 3 points on a pair of surfaces, there is a 1-1 correspondence between the set of surface diffeomorphisms between them and the set of Beltrami coefficients on the source domain. Hence, every bijective surface map can be represented by a unique Beltrami coefficient. Conversely, given a Beltrami coefficient, we can reconstruct the unique surface map associated to it using the Beltrami Holomorphic flow (BHF) method introduced in this paper. Using this representation, 1/3 of the storage space is saved. We can further reduce the storage requirement by 90% by compressing the Beltrami coefficients using Fourier approximations. We test our algorithm on synthetic data, real human brain and hippocampal surfaces. Our results show high accuracy in the reconstructed data, while the amount of storage is greatly reduced. Our approach is compared with the Fourier compression of the coordinate functions using the same amount of data. The latter approach often shows jaggy results and cannot guarantee to preserve diffeomorphisms.

I. Introduction

In computer vision and medical imaging, it is crucial to look for 1-1 correspondences between surfaces for further analysis. Such process is called surface registration. Surface maps computed from registration processes are usually represented and stored as 3D functions in $\mathbb{R}^3$. A huge storage memory is required, especially when a large set of fine surface are to be analyzed. It causes problems for data transmission and storage. This problem is particularly common in medical imaging, in which a large set of data has to be considered. Usually, a great amount of memory and bandwidth are needed to store and transmit the data of surface maps. In fact, this research was initially motivated by an actual situation in Brain Mapping research. In a project to analyze the hippocampal shape difference in patients with or without Alzheimer's disease, a thousand of hippocampal surfaces have to be registered. In order to study their time-dependent shape changes, each initial surface has to be mapped onto several other surfaces taken at different future times. Furthermore, several maps have to be constructed between each surface pair to satisfy different matching criteria. With a typical surface mesh size of 50k vertices, the storage requirement could easily exceed 10 gigabytes, making storing and sharing surface map data a great inconvenience. Nevertheless, very little work has been done on the compression of bijective surface maps. This motivates us to look for a simple representation of surface diffeomorphisms that significantly reduces the required storage memory.

In this work, we propose a simple representation of surface maps using the *Beltrami coefficients*. The Beltrami coefficient is a complex-valued function defined on surfaces with supreme norm strictly less than 1. It measures the local conformality distortion of surface maps. Every surface map is associated with a Beltrami coefficient. According to the Quasi-conformal Teichmüller theory, fixing any 3 points, there is an 1-1 correspondence between the set of surface diffeomorphisms and the set of Beltrami coefficients on the source domain. In other words, every surface map can be represented by a unique Beltrami coefficient. Conversely, given a Beltrami coefficient, we can reconstruct the unique surface map associated to it. The Beltrami coefficient is a simple representation that captures many important information of the map. In this paper, we propose the *Beltrami Holomorphic flow* (BHF) method to iteratively reconstruct the surface map associated with a given Beltrami coefficient. Using this representation, 1/3 of the required storage

space is saved. Also, the Beltrami coefficient has very little constraints. The only constraint is that its supreme norm is strictly less than 1. It does not have any requirement of injectivity nor subjectivity. This allows us to further compress the Beltrami coefficient using Fourier approximations, which can further reduce the storage requirement by 90%. Fourier compression is not possible for other representations such as 3D coordinate functions, as the diffeomorphic property (1-1 and onto) of the resulting maps cannot be guaranteed (see Figure 3, 6, 9).

The contribution of this paper is three-fold: 1. We propose the computation of Beltrami coefficients to represent bijective surface maps; 2. We propose the Beltrami Holomorphic flow (BHF) method to reconstruct surface maps from their Beltrami coefficients; 3. We propose the further compression of Beltrami coefficients by Fourier approximations, which further reduce the storage requirement by 90%.

This paper is laid out as follow. In Section 2, we describe the relevant works closely related to this research. In Section 3, we describe some basic mathematical concepts related to our algorithms. In Section 4, we describe in detail the main algorithms we use to represent and compress surface diffeomorphisms with Beltrami coefficients. We also describe how surface maps can be reconstructed from Beltrami coefficients. Experimental results are shown in Section 5. In Section 6, we draw a conclusion and describe possible future work.

II. Related works

Surface registration has been studied extensively and different representations of surface maps have been proposed. Conformal parameterizations have been widely used [2], [4], [5], [6], [7], [15]. For example, Gu et al. [4], [5], [15] proposed to compute the conformal parameterizations of human brain surfaces for registration using harmonic energy minimization and holomorphic 1-forms. Hurdal et al. [7] proposed to compute the conformal parameterizations using circle packing and applied it to registration of human brains. To obtain landmark matching surface registrations, Wang et al. [14] proposed to compute the optimized conformal parameterizations of brain surfaces by minimizing a compounded energy. All of the above algorithms represent surface maps with their 3D coordinate functions. Lui et al. [12] proposed the use of vector fields to represent surface maps and reconstruct them through integral flow equations. They obtained shape-based landmark matching harmonic maps by looking for the best vector fields minimizing a shape energy. The use of vector fields to represent surface maps makes optimization easier, but they cannot describe all surface maps. Time dependent vector fields can be used to represent the set of all surface maps. For example, Joshi et al. [9] proposed the generation of large deformation diffeomorphisms for landmark point matching, where the registrations are generated as solutions to the transport equation of time dependent vector fields. The time dependent vector fields facilitate the optimization procedure, although it may not be a good representation of surface maps since it requires more memory.

Compression of mappings has also been studied. Chai et al. [1] proposed the depth map compression algorithm by encoding mapppings as a simplified triangular meshes. Lewis [11] described a technique for compressing surface potential mapping data using transform techniques. All these methods deal with the compression of real-valued functions defined on 2D domains. For vector-valued functions, Stachera et al. [13] developed an algorithm to compress normal maps by decomposing them in the frequency domain. Ioup [8] also proposed to compress vector map data in the frequency domain. Kolesnikov et al. [10] proposed an algorithm for distortion-constrained compression of vector maps, based on optimal polygonal approximations and dynamic quantizations of vector data. All these methods do not deal with preverving bijective maps between surfaces. The bijectivity (1-1, onto) of the maps can be easily lost due to lossy compression.

III. Theoretical Background

In this section, we describe some basic mathematical concepts related to our algorithms.

A surface S with a conformal structure is called a *Riemann surface*. Given two Riemann surfaces M and N, a map $f : M \to N$ is *conformal* if it preserves the surface metric up to a multiplicative factor

called the conformal factor. An immediate consequence is that every conformal map preserves angles. With the angle-preserving property, a conformal map effectively preserves the local geometry of the surface structure.

A generalization of conformal maps is the *quasi-conformal* maps, which are orientation-preserving homeomorphisms between Riemann surfaces with bounded conformality distortion, in the sense that their first order approximations takes small circles to small ellipses of bounded eccentricity [3]. Thus, a conformal homeomorphism that maps a small circle to a small circle can also be regarded as quasi-conformal. Mathematically, $f\colon \mathbb{C} \to \mathbb{C}$ is quasi-conformal provided that it satisfies the Beltrami equation:

$$\frac{\partial f}{\partial \overline{z}} = \mu(z)\frac{\partial f}{\partial z}. \tag{1}$$

for some complex valued Lebesgue measurable μ satisfying $||\mu||_\infty < 1$. In terms of the metric tensor, consider the effect of the pullback under f of the usual Euclidean metric ds_E^2; the resulting metric is given by:

$$f^*(ds_E^2) = |\frac{\partial f}{\partial z}|^2 |dz + \mu(z)d\overline{z}|^2. \tag{2}$$

which, relative to the background Euclidean metric dz and $d\overline{z}$, has eigenvalues $(1+|\mu|)^2\frac{\partial f}{\partial z}$ and $(1-|\mu|)^2\frac{\partial f}{\partial z}$. μ is called the *Beltrami coefficient*, which is a measure of non-conformality. In particular, the map f is conformal around a small neighborhood of p when $\mu(p) = 0$. Infinitesimally, around a point p, f may be expressed with respect to its local parameter as follows:

$$\begin{aligned} f(z) &= f(p) + f_z(p)z + f_{\overline{z}}(p)\overline{z} \\ &= f(p) + f_z(p)(z + \mu(p)\overline{z}). \end{aligned} \tag{3}$$

Obviously, f is not conformal if and only if $\mu(p) \neq 0$. Inside the local parameter domain, f may be considered as a map composed of a translation to $f(p)$ together with a stretch map $S(z) = z + \mu(p)\overline{z}$, which is postcomposed by a multiplication of $f_z(p)$, which is conformal. All the conformal distortion of $S(z)$ is caused by $\mu(p)$. $S(z)$ is the map that causes f to map a small circle to a small ellipse. From $\mu(p)$, we can determine the angles of the directions of maximal magnification and shrinking and the amount of them as well. Specifically, the angle of maximal magnification is $\arg(\mu(p))/2$ with magnifying factor $1 + |\mu(p)|$; The angle of maximal shrinking is the orthogonal angle $(\arg(\mu(p)) - \pi)/2$ with shrinking factor $1 - |\mu(p)|$. The distortion or dilation is given by:

$$K = 1 + |\mu(p)|/1 - |\mu(p)|. \tag{4}$$

Thus, the Beltrami coefficient μ gives us all the information about the properties of the map (See Figure 1). According to Teichmüller Quasiconformal theory, there is a 1-1 correspondence between the set of Beltrami differentials and the set of diffeomorphisms $f\colon S_1 \to S_2$ fixing three points. In other word, Beltrami coefficients give us a simple way to represent surface maps.

IV. Main Algorithms

In this section, we describe in detail the main algorithms we use to represent and compress surface diffeomorphisms with Beltrami coefficients. We also describe how a surface map can be reconstructed from its Beltrami coefficient.

A. Surface Map Representation using Beltrami Coefficients

In computer vision and medical imaging, it is crucial to look for an 1-1 correspondence between surfaces for further analysis. Surface registration is commonly represented by 3D coordinate functions in $\mathbb{R}^3$. This representation requires lots of storage space and is difficult to manipulate. For example, the 3D coordinate functions have to a satisfy certain constraint on the Jacobian J (namely, $J > 0$) in order to preserve the 1-1 correspondence of the surface maps. Enforcing this constraint adds extra difficulty in manipulating and

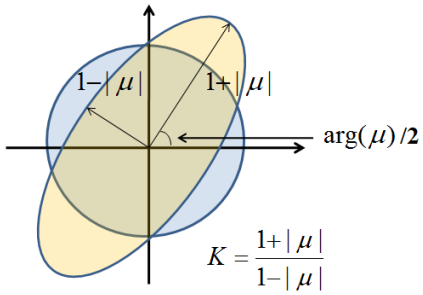

Fig. 1. Illustration of how the Beltrami coefficient μ measures the distortion of a quasi-conformal mapping that maps a small circle to an ellipse with dilation K.

adjusting surface maps. It is therefore important to have a simpler representation with as few constraints as possible.

Given two surfaces S_1 and S_2 with the same topology. According to the Teichmüller Quasiconformal theory, there is a 1-1 correspondence between the set of Beltrami differentials and the set of diffeomorphisms $f\colon S_1 \to S_2$ fixing three points [3]. In other words, given any surface diffeomorphism $f^\mu\colon S_1 \to S_2$ and 3-point correspondence, we can represent f^μ with a uniquely determined Beltrami differential $\mu\frac{\overline{dz}}{dz}$. Beltrami differential is defined on every coordinate patch. For genus 0 closed surfaces or simply connected open surfaces, they can be conformally parameterized with a single global patch [4], [5], [15]. Beltrami coefficients can then be used instead of Beltrami differentials. The Beltrami coefficient μ is a complex-valued functions defined on S_1 with $\sup|\mu| < 1$. There are no restrictions on μ that it has to be 1-1, surjective or satisfy some constraints on the Jacobian. With this representation, we can easily manipulate surface maps.

Suppose S_1 and S_2 are both either genus 0 closed surfaces or simply connected open surfaces. Let $f\colon S_1 \to S_2$, and suppose 3 points $\{p_1, p_2, p_3\}$ on S_1 correspond to 3 points on S_2 by $\{p_1, p_2, p_3\} \leftrightarrow \{q_1 = f(p_1), q_2 = f(p_2), q_3 = f(p_3)\}$. S_1 and S_2 can be conformally parameterized with a global patch. Denote the parameterizations by $\phi_1\colon S_1 \to D$ and $\phi_2\colon S_2 \to D$, where D is either a unit sphere $\mathbb{S}^2$ or a 2D rectangle. We fix $\{p_1, p_2, p_3\}$ and $\{q_1, q_2, q_3\}$ to consistent locations on the parameter domain. For example, in the case that $D = \mathbb{S}^2$, we map $\{p_1, p_2, p_3\}$ and $\{q_1, q_2, q_3\}$ to 0 (north pole), 1 and ∞ (south pole) respectively. Here, we have identified $\mathbb{S}^2$ with the extended complex plane $\mathbb{C}^*$. Now, we can compute the Beltrami coefficient μ_f associated uniquely to f to represent f. The Beltrami coefficient μ_f can be computed by considering the composition map $\widetilde{f} = \phi_2 \circ f \circ \phi_1^{-1}\colon D \to D$. Mathematically, μ_f is given by the following formula:

$$\mu_f = \frac{\partial \widetilde{f}}{\partial \overline{z}} / \frac{\partial \widetilde{f}}{\partial z} = \frac{1}{2}\left(\frac{\partial \widetilde{f}}{\partial x} + \sqrt{-1}\frac{\partial \widetilde{f}}{\partial y}\right) / \frac{1}{2}\left(\frac{\partial \widetilde{f}}{\partial x} - \sqrt{-1}\frac{\partial \widetilde{f}}{\partial y}\right).$$

In practice, surfaces are commonly approximated by discrete meshes comprising of triangular or rectangular faces. The parameterizations map the surface meshes onto the mesh D in $\mathbb{C}$. The partial derivatives (or gradient) can be discretely approximated on each face of D. By taking average, the partial derivatives and hence the Beltrami coefficient can be computed on each vertex.

The Beltrami coefficient consists of two real functions only, namely the real and imaginary parts. Compared to the representation using 3D coordinate functions, this representation reduces 1/3 of the original storage space.

B. Reconstruction of Surface Maps

Given the Beltrami coefficient μ defined on S_1. We propose the *Beltrami Holomorphic flow* (BHF) method to reconstruct the surface diffeomorphism $f^\mu\colon S_1 \to S_2$ associated with μ. The BHF iteratively flows the identity map to f^μ. In this subsection, we describe the BHF method in detail.

The variation of f^μ under the variation of μ can be expressed explicitly. Suppose $\widetilde{\mu}(z) = \mu(z) + t\nu(z) + \mathcal{O}(t^2)$. Then, $f^{\widetilde{\mu}(z)}(w) = f^\mu(w) + tV(f^\mu, \nu)(w) + \mathcal{O}(t^2)$, where

$$V(f^\mu, \nu)(w) = -\frac{f^\mu(w)(f^\mu(w)-1)}{\pi} \times \int_D \frac{\nu(z)(f^\mu_z(z))^2 dxdy}{f^\mu(z)(f^\mu(z)-1)(f^\mu(z)-f^\mu(w))}. \tag{5}$$

Using this fact, we propose the BHF method to iteratively flow the identity map to f^μ. Given the parameterizations $\phi_1 \colon S_1 \to D$ and $\phi_2 \colon S_2 \to D$, we look for the map $\widetilde{f}^\mu = \phi_2 \circ f^\mu \circ \phi_1^{-1} \colon D \to D$ associated uniquely with $\widetilde{\mu} = \mu \circ \phi_1^{-1} \colon D \to \mathbb{C}$. f^μ can then be obtained by $f^\mu = \phi_2^{-1} \circ \widetilde{f}^\mu \circ \phi_1$.

We start with the identity map $\mathbf{Id}$ of which the Beltrami coefficient is equal to 0. Let N be the number of iterations. Define $\widetilde{\mu}_k = k\widetilde{\mu}/N$, $k = \{0, 1, 2, ..., N\}$. Let $\widetilde{f}^{\widetilde{\mu}_k}$ be the map associated with $\widetilde{\mu}_k$. Note that $\widetilde{f}^{\widetilde{\mu}_0} = \mathbf{Id}$ and $\widetilde{f}^{\widetilde{\mu}_N} = \widetilde{f}^\mu$. Equation 5 allows us to iteratively compute $\widetilde{f}^{\widetilde{\mu}_k}$ and thus obtain a sequence of maps flowing from $\mathbf{Id}$ to $\widetilde{f}^\mu$. Mathematically, the iterative scheme is given by:

$$\widetilde{f}^{\widetilde{\mu}_{k+1}} = \widetilde{f}^{\widetilde{\mu}_k} + \frac{1}{N} V(\widetilde{f}^{\widetilde{\mu}_k}, \widetilde{\mu}); \quad \widetilde{f}^{\widetilde{\mu}_0} = \mathbf{Id} \tag{6}$$

BHF computes a sequence of surface maps $\{\widetilde{f}^{\widetilde{\mu}_k}\}$ converging to $\widetilde{f}^\mu$. The approximation of $\widetilde{f}^{\widetilde{\mu}_k}$ is more accurate with a smaller time step or equivalently a larger number of iterations N. In practice, the approximations are very accurate when $N \geq 15$ (see Figure 13). In our experiments, we set $N = 20$.

C. Fourier Compression of Beltrami Coefficients

The Beltrami coefficient can be further compressed using Fourier approximations to reduce the storage space. An important consideration is to preserve the diffeomorphic property of the surface map after the compression. Under the representation by coordinate functions, the Jacobian has to be greater than 0 in order to ensure the diffeomorphic property. This constraint is equivalent to an inequality in the partial derivatives of the coordinate functions. Enforcing this constraint is difficult during compression and the diffeomorphic property is easily lost (see Figure 3, 6, 9). The representation by Beltrami coefficient, however, is advantageous because it does not have any requirement for injectivity and subjectivity, making the Jacobian constraint unnecessary. The only requirement for the Beltrami coefficient μ is that it has to be a complex-valued function defined on the surface with supreme norm less than 1. We can therefore compress μ using Fourier approximations without losing the diffeomorphic property.

The Beltrami coefficient μ can be approximated as follow:

$$\mu(x, y) = \sum_{j,k=-N}^{N} c_{j,k} e^{\sqrt{-1}\pi jx/T} e^{\sqrt{-1}\pi ky/T},$$

where

$$c_{j,k} = \frac{1}{4T^2} \int_{-T}^{T} \int_{-T}^{T} \mu(x, y) e^{-\sqrt{-1}\pi jx/T} e^{-\sqrt{-1}\pi ky/T} dxdy.$$

We can use fast Fourier transform to compute the coefficients $c_{j,k}$ efficiently. In practice, we set $N = 20$ and the approximation is already very accurate (see Figure 11). The Fourier compression significantly reduces the storage required to 10% of the original data size. Experimental results show that the compression of μ is stable and effective.

V. Experimental Results

We test our algorithm on synthetic surface data, real human brain surfaces and real hippocampal surfaces. Experimental results show that our algorithm is effective and stable.

Figure 2 shows the representation of a diffeomorphism from the unit square to itself using the Beltrami coefficient. (A) shows the original diffeomorphism. (B) shows the norm of the Beltrami coefficient representing the map. (C) shows the reconstructed map from the Beltrami coefficient. The dots represent the exact values of the original map. Note that the reconstructed map closely matches the original map. (D) shows the errors of the reconstructed maps versus the number of iterations under the Beltrami Holomorphic flow (BHF), which are defined as

$$Error = \sup ||f^{Re} - f||, \tag{7}$$

where f^{Re} is the reconstructed map. After 20 iterations, the BHF reconstructed map closely approximates the original map.

Figure 3(A) shows the Fourier compression result of the Beltrami coefficient μ. We take $N = 15$ in the Fourier series approximation. The reconstructed map closely matches the original map (see dots) as well. (B) shows the Fourier compression result of the coordinate functions. The Jacobian constraint is not satisfied under the compression. The diffeomorphic property is lost. Figure 4 shows the Fourier compression result of μ with $N = 5, 10, 15, 20$ respectively. The accuracy improves rapidly with increasingly larger N's.

We also test our algorithm on real cortical hemispheric surfaces extracted from brain MRI scans, acquired from normal and unhealthy subjects at 1.5 T (on a GE Sigma scanner). Figure 5(A) shows two different brain surfaces and a surface map between them. The surface map can be represented by the Beltrami coefficient. (B) shows the colormap of the norm of the Beltrami coefficient. (C) shows the reconstructed surface map from the Beltrami coefficient. The black dots represent the exact values of the original surface map. The result shows that the reconstruction of the surface map from the Beltrami coefficient is very accurate.

Figure 6 shows the Fourier compression results for the brain surfaces. (A) and (B) show two brains and a surface map between them. (C) shows the Fourier compression result of the coordinate functions. Note that the diffeomorphic property is greatly distorted. (D) shows the Fourier compression result of the Beltrami coefficient with $N = 20$. The reconstructed map accurately approximates the original map (see black dots). Figure 7 shows the Fourier compression results of μ for the brain surfaces with $N = 5, 10, 15$ and 20 respectively. Again, the error reduces rapidly as N increases.

In Figure 8, we test our algorithm on real hippocampal surfaces, which is an important brain structure for the study of Alzheimer's disease. (A) shows two different hippocampal surfaces and a surface diffeomorphism between them. We represent the surface map with the Beltrami coefficient and the colormap of its norm is shown in (B). (C) shows the reconstructed map from the Beltrami coefficient. Again, the black dots represent the exact location under the original map. The error as defined in Equation 7 versus the number of iterations during the Beltrami Holomorphic Flow (BHF) is as shown in (D). Figure 9 shows the Fourier compression result of the 3D coordinate functions for the hippocampal surfaces. Note that the diffeomorphic property cannot be preserved under the compression. The Fourier compression results of the Beltrami coefficient for the hippocampal surfaces with $N = 5, 10, 15, 20$ are shown in Figure 10.

We have also analyzed our proposed algorithm quantitatively. Figure 11 shows the error of the reconstructed diffeomorphism under the Fourier compression versus the number of Fourier coefficients. Let f^{Re} be the reconstructed surface map and f be the original surface map. The errors of the reconstructed maps as defined by Equation 7 are shown in Figure 11. The blue curve shows the errors of the reconstructed diffeomorphisms under the Fourier compression of the Beltrami coefficient. The error decreases rapidly as the number of Fourier coefficients increases. The red curve shows the errors of the reconstructed diffeomorphisms under the Fourier compression of the coordinate functions. The error is much greater than the Fourier compression of the Beltrami coefficient.

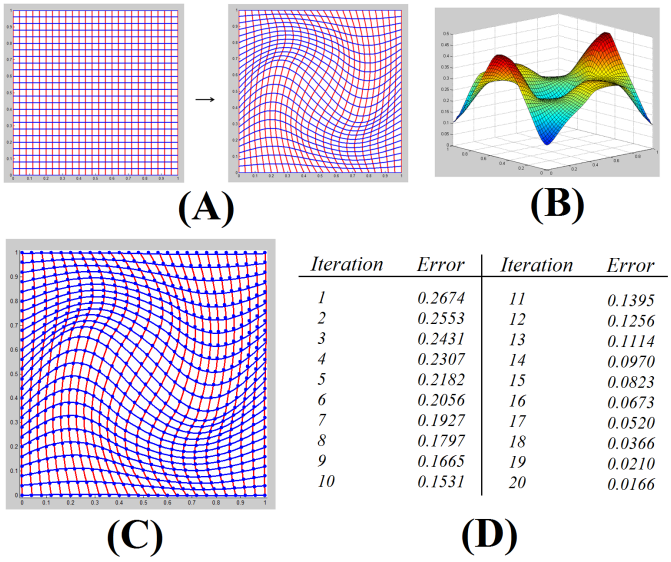

Iteration	Error	Iteration	Error
1	0.2674	11	0.1395
2	0.2553	12	0.1256
3	0.2431	13	0.1114
4	0.2307	14	0.0970
5	0.2182	15	0.0823
6	0.2056	16	0.0673
7	0.1927	17	0.0520
8	0.1797	18	0.0366
9	0.1665	19	0.0210
10	0.1531	20	0.0166

Fig. 2. Reconstruction of the diffeomorphism of a 2D domain from the Beltrami coefficient using Beltrami Holomorphic flow (BHF).

To analyze quantitatively how well the diffeomorphic property is preserved under our algorithm, we compute a measure called the *inverse Jacobian measure*. It is defined as: $\text{Inv}(J) = \sup |1 - \frac{J}{J^{Re}}|$, where J^{Re} is the Jacobian of the reconstructed map and J is the Jacobian of the original map. J^{Re} is small when overlapping occurs. Thus, a large value of $\text{Inv}(J)$ means an occurrence of overlapping in f^{Re} and a big deviation of f^{Re} from f. Figure 12 shows the values of $\text{Inv}(J)$ versus the number of coefficients used under the Fourier compression of the coordinate functions and the Beltrami coefficient respectively. The red curve shows the values of $\text{Inv}(J)$ under the Fourier compression of the coordinate functions versus the number of Fourier coefficients used. Note that the values of $\text{Inv}(J)$ are quite big, meaning that overlapping occurs in f^{Re} and the diffeomorphic property is seriously distorted. The blue curve shows the values of $\text{Inv}(J)$ under the Fourier compression of the Beltrami coefficient versus the number of Fourier coefficients used. The values of $\text{Inv}(J)$ are very small, meaning that f^{Re} preserves the diffeomorphic property well and reconstructs the original map f accurately.

To examine how many iterations are needed in the Beltrami Holomorphic flow process, we plot in Figure 13 the error of f^{Re} versus the number of iterations used in the BHF process. The blue curve represents the errors of f^{Re} versus the number of iterations used without the Fourier compression of μ. The red curve represents the errors of f^{Re} versus the number of iterations used with the Fourier compression of μ. In both cases, the error of f^{Re} decreases rapidly with more iterations used in the BHF process. The error stabilizes when the number of iterations is about 20.

VI. Conclusion and Future Work

In this paper, we address the problem of finding a simple representation of surface maps that significantly reduces the required storage memory. It is especially important in medical imaging, in which a large set of surfaces have to be registered. A great amount of storage capacity and bandwidth are needed to store and transmit the surface map data. Hence, an algorithm for compressing surface maps is of utmost importance. We propose a novel representation of surface maps using Beltrami coefficients. Fixing any 3 points, there is a 1-1 correspondence between the set of surface diffeomorphisms and the set of Beltrami coefficients. We propose the Beltrami Holomorphic flow (BHF) method to iteratively reconstruct the surface map with a given Beltrami coefficient. Using the Beltrami coefficient to represent the surface map reduces 1/3 of the required storage space. We can further compress the Beltrami coefficient using the Fourier approximation, which significantly reduces the storage required by 90% further. Experimental results on synthetic data, real human brain data and real hippocampus surfaces show that our method is stable and effective in

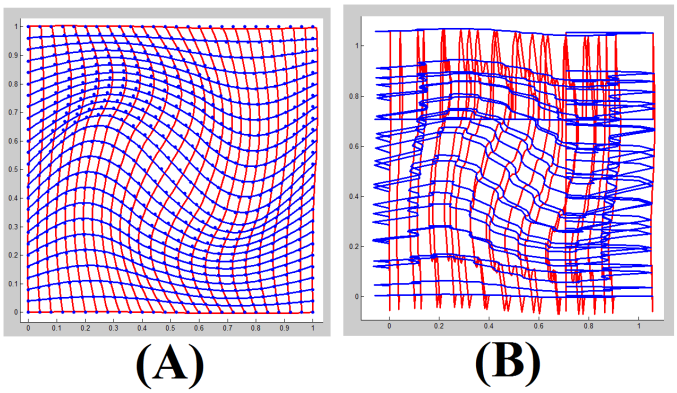

Fig. 3. (A) shows the Fourier compression result of the Beltrami coefficient; (B) shows the Fourier compression result of the coordinate functions

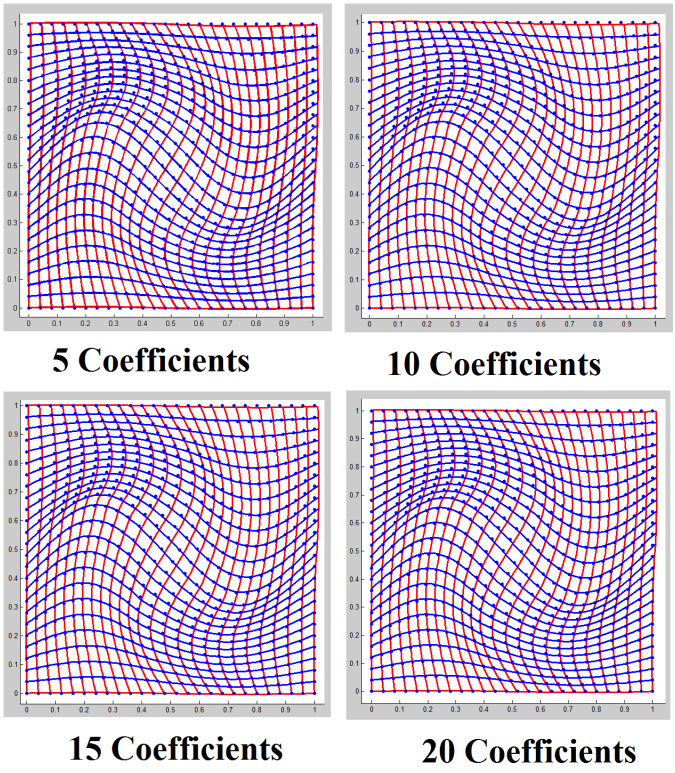

Fig. 4. The results from Fourier compression of μ with $N = 5, 10, 15$ and 20.

accurately representing surface maps and requires less storage memory. In the future, we will apply the algorithm to represent and compress surface maps obtained during the surface registration process in our medical research.

Acknowldgement:: PT is supported by NIH: EB008432, EB008281, EB007813, HD050735 & AG036535. TC is supported by NSF GEO-0610079, NSF IIS-0914580, NIH U54 RR021813 and ONR N00014-09-1-0105. XG is supported by NIH 1R01EB0075300A1, NSF IIS 0916286, CCF0916235, CCF0830550, III0713145, and ONR N000140910228.

REFERENCES

[1] B.-B. Chai, S. Sethuraman, H. S. Sawhney, and P. Hatrack. Depth map compression for real-time view-based rendering. *Pattern Recognition Letters*, 25:755–766, 2004.

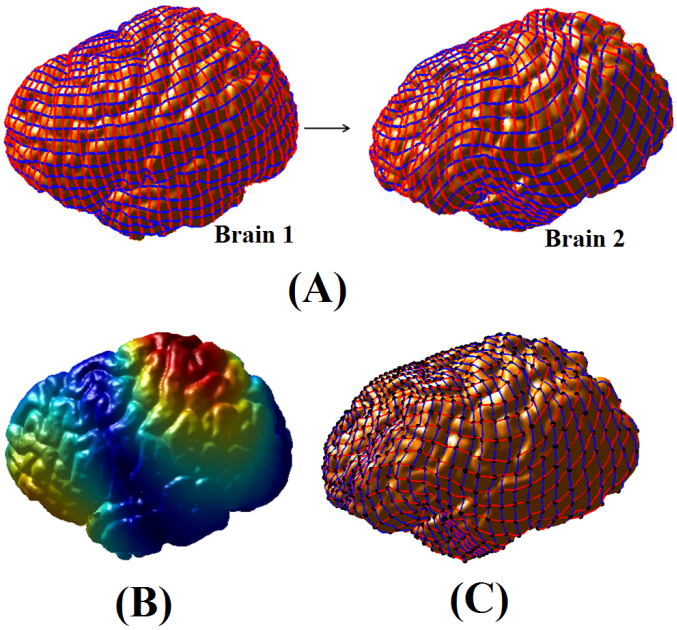

Fig. 5. Reconstruction of a surface diffeomorphism between real human brain surfaces from its Beltrami coefficient.

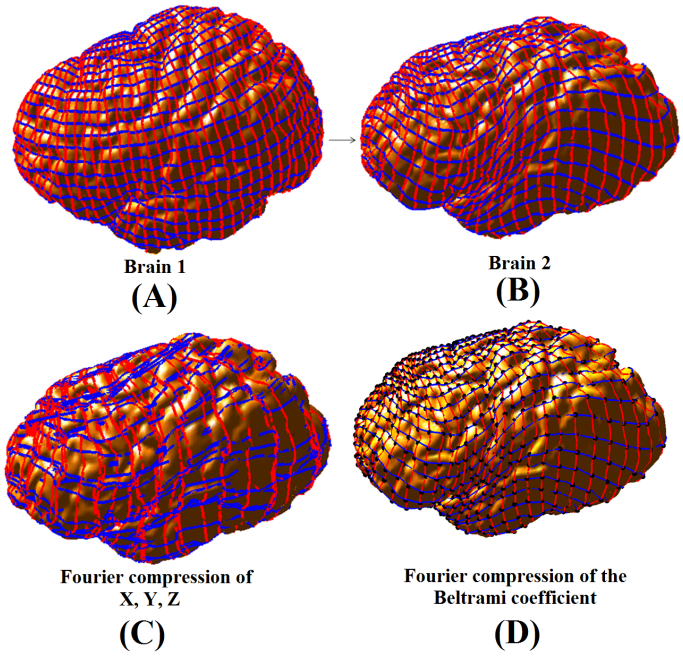

Fig. 6. The Fourier compression results for a brain surface diffeomorphism. (A) and (B) show two human brains and a surface map between them. (C) shows the Fourier compression result of its 3D coordinate functions. (D) shows the Fourier compression result of the Beltrami coefficient with $N = 20$

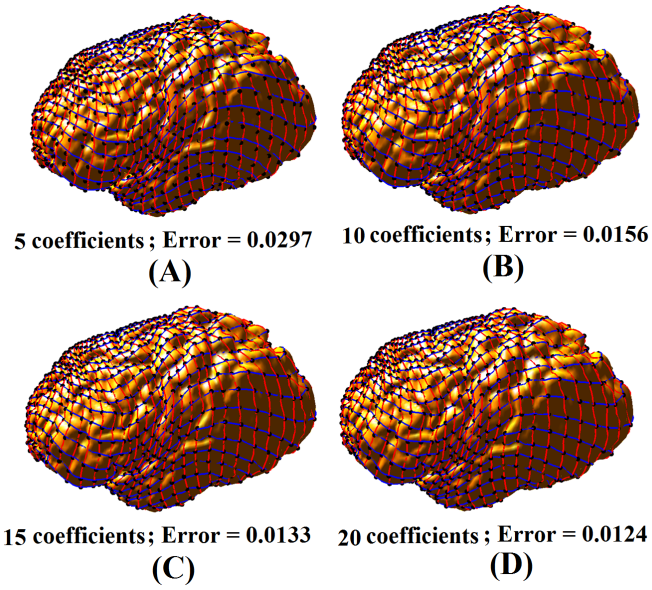

Fig. 7. The results of Fourier compression of μ for a brain surface diffeomorphism with $N = 5, 10, 15$ and 20.

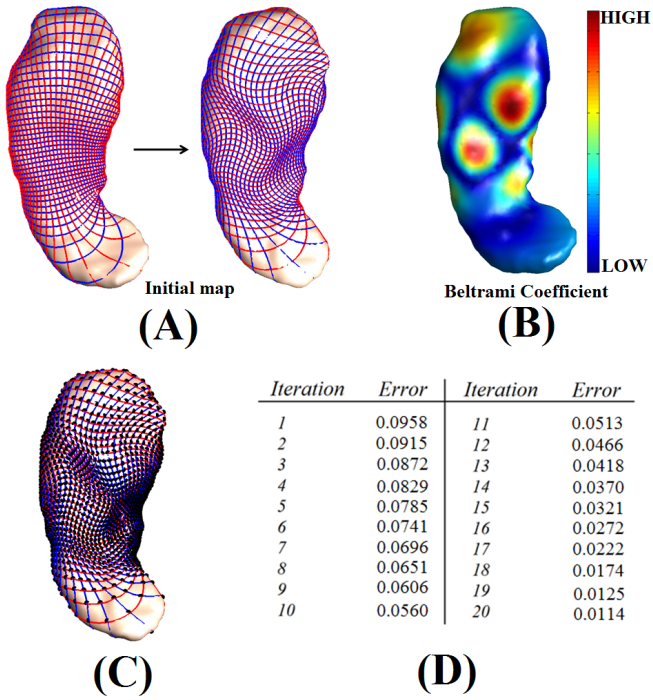

Iteration	*Error*	*Iteration*	*Error*
1	0.0958	*11*	0.0513
2	0.0915	*12*	0.0466
3	0.0872	*13*	0.0418
4	0.0829	*14*	0.0370
5	0.0785	*15*	0.0321
6	0.0741	*16*	0.0272
7	0.0696	*17*	0.0222
8	0.0651	*18*	0.0174
9	0.0606	*19*	0.0125
10	0.0560	*20*	0.0114

Fig. 8. (A) shows two different hippocampal surfaces and a surface diffeomorphism between them. We represent the surface map with its Beltrami coefficient and the colormap of its norm is shown in (B). (C) shows the reconstructed map from the Beltrami coefficient. (D) shows the errors of the intermediate maps during Beltrami Holomorphic Flow (BHF).

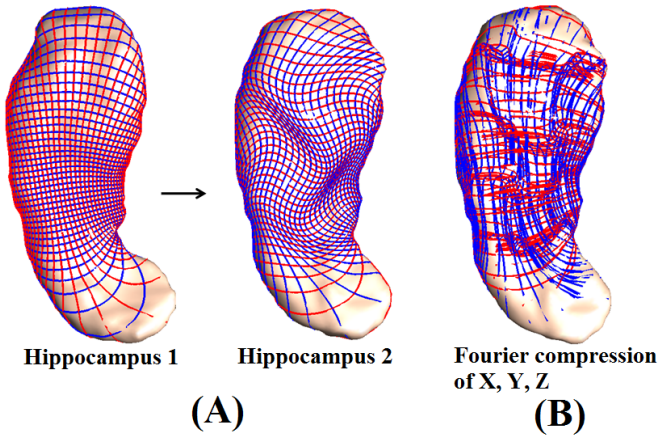

Fig. 9. The Fourier compression result of the 3D coordinate functions for hippocampal surfaces.

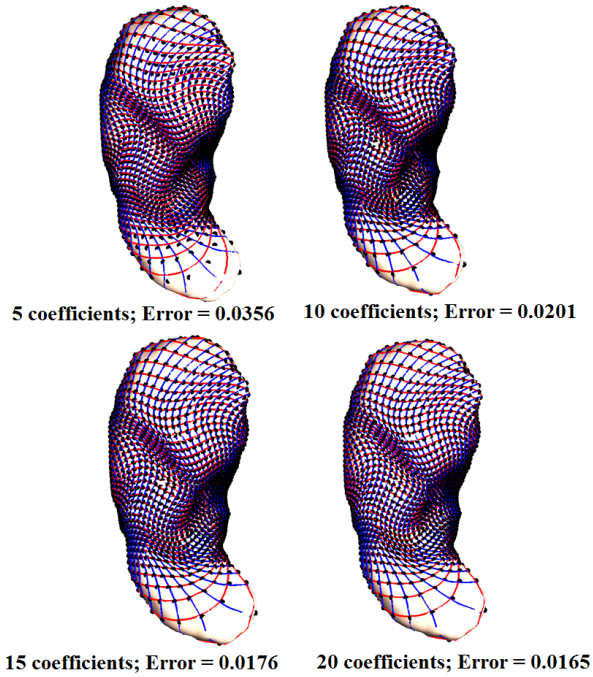

Fig. 10. The Fourier compression results of the Beltrami coefficient for a hippocampal surface diffeomorphism with $N = 5, 10, 15$ and 20

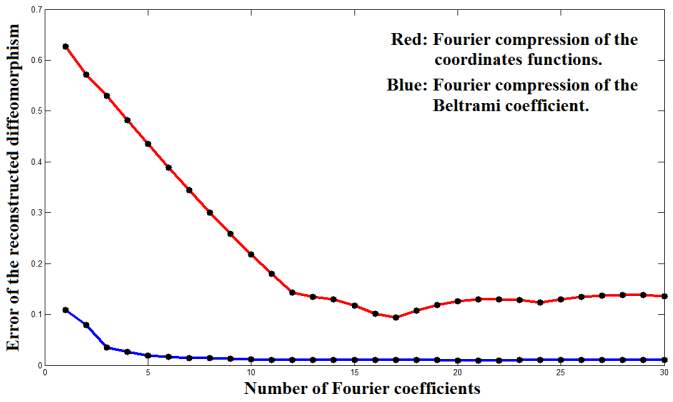

Fig. 11. The errors of the reconstructed diffeomorphisms under the Fourier compression versus the number of Fourier coefficients used.

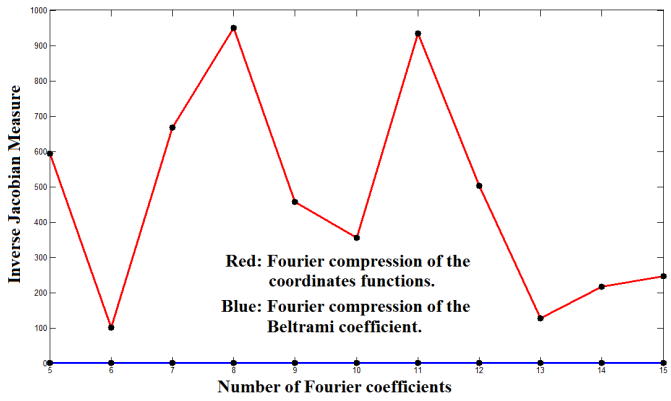

Fig. 12. The values of $\mathrm{Inv}(J)$ under the Fourier compression of the coordinate functions and the Beltrami coefficient.

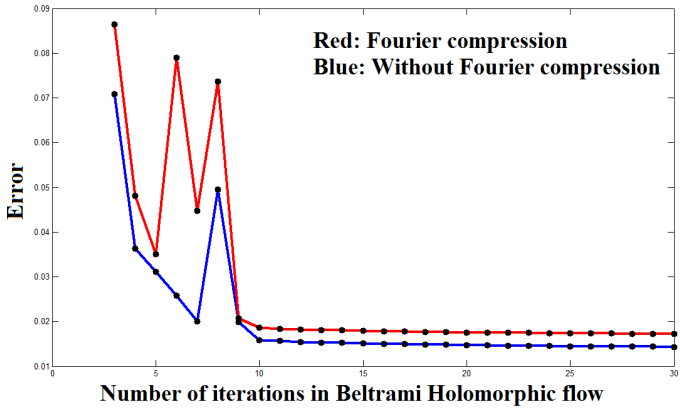

Fig. 13. The error of f^{Re} versus the number of iterations used in the BHF process.

[2] B. Fischl, M. Sereno, R. Tootell, and A. Dale. High-resolution intersubject averaging and a coordinate system for the cortical surface. *Human Brain Mapping*, 8:272–284, 1999.

[3] F. Gardiner and N. Lakic. *Quasiconformal Teichmuller Theory*. American Mathematics Society, 2000.

[4] X. Gu, Y. Wang, T. F. Chan, P. M. Thompson, and S.-T. Yau. Genus zero surface conformal mapping and its application to brain surface mapping. *IEEE Transactions on Medical Imaging*, 23(8):949–958, 2004.

[5] X. Gu and S. Yau. Computing conformal structures of surfaces. *Communication in Information System*, 2(2):121–146, 2002.

[6] S. Haker, S. Angenent, A. Tannenbaum, R. Kikinis, G. Sapiro, and M. Halle. Conformal surface parameterization for texture mapping. *IEEE Transaction of Visualization and Computer Graphics*, 6:181–189, 2000.

[7] M. K. Hurdal and K. Stephenson. Discrete conformal methods for cortical brain flattening. *Neuroimage*, 45:86–98, 2009.

[8] J. W. Ioup, M. L. Gendron, and M. C. Lohrenz. Vector map data compression with wavelets. *Journal of Navigation*, 53:437–449, 2000.

[9] S. Joshi and M. Miller. Landmark matching via large deformation diffeomorphisms. *IEEE Transactions on Image Processing*, 9(8):1357–1370, 2000.

[10] A. Kolesnikov and A. Akimov. Distortion-constrained compression of vector maps. *Proceedings of the 2007 ACM symposium on Applied computing*, pages 8–12, 2007.

[11] J. Lewis and M. English. Compression of body surface potential maps using image compression techniques. *Proceeding of Computers in Cardiology*, pages 401–404, 1995.

[12] L. Lui, S. Thiruvenkadam, Y. Wang, T. Chan, and P. Thompson. Optimized conformal parameterization of cortical surfaces using shape based matching of landmark curves. *Proceeding in Medical Image Computing and Computer-Assisted Internvention - MICCAI 2005*, pages 494–502, 2008.

[13] J. Stachera and P. Rokita. Normal map compression based on *btc* and wavelet coding. *Proceeding of Real-Time Image Processing*, 6811:68110S–68110S–8, 2008.

[14] Y. Wang, L. Lui, T. Chan, and P. Thompson. Optimization of brain conformal mapping with landmarks. *Proceeding in Medical Image Computing and Computer-Assisted Internvention - MICCAI 2005*, pages 675–683, 2005.

[15] Y. Wang, L. M. Lui, X. Gu, K. M. Hayashi, T. F. Chan, A. W. Toga, P. M. Thompson, and S.-T. Yau. Brain surface conformal parameterization using riemann surface structure. *IEEE Transactions on Medical Imaging*, 26(6):853–865, 2007.